

CrossMark
click for updatesCite this: *J. Mater. Chem. A*, 2016, 4, 14968Received 2nd July 2016
Accepted 2nd September 2016

DOI: 10.1039/c6ta05545a

www.rsc.org/MaterialsA

A three-dimensionally stretchable high performance supercapacitor†

Sisi He,^a Longbin Qiu,^a Lie Wang,^a Jingyu Cao,^a Songlin Xie,^a Qiang Gao,^{ab} Zhitao Zhang,^a Jing Zhang,^a Bingjie Wang^{*a} and Huisheng Peng^{*a}

A three-dimensionally stretchable supercapacitor is created by designing a novel pyramid structure without the use of an elastic substrate. Compared with previous stretchable supercapacitors that may deform in plane on elastic substrates, these pyramid-structured supercapacitors can be stretched in three dimensions with high stability. Their electrochemical performances are well maintained after stretching in three dimensions for thousands of cycles, and they show both higher energy and power densities compared with the other reported stretchable supercapacitors. In addition, they are breathable due to the designed grooves that produce the pyramid structure, which is particularly promising for many emerging applications such as wearable electronics. This work further provides an effective strategy for developing next-generation flexible electronic devices with high performances.

Introduction

Stretchable energy storage devices have been developed to meet the requirement of pervasive portable electronic devices, such as the recently developed epidermal electronics.^{1–8} To date, stretchable energy storage devices are generally realized by depositing electrodes and active materials onto a pre-stretched elastic polymer substrate to form a waved structure.^{9–14} However, the elastic substrate adds extra weight and volume to the device without contribution to the electrochemical storage capability. In addition, this method may be applicable to limited materials that possess high flexibility and can adhere well to the substrate.

On one hand, the resulting fiber-shaped energy storage devices are stretchable along the axial direction, while the planar and textile-type ones can be stretched in plane.^{7,15–21} On

the other hand, the modern electronic devices tend to be integrated into complex systems like elbows and knees that are required to work under stretching in three dimensions.^{22–28} However, for the available stretchable energy storage devices, they failed to work when they underwent stretching out of the plane as the two electrodes would come into contact with each other and induce a short circuit. Therefore, it is urgent to design and produce energy storage devices that can effectively work under three-dimensional stretching.

Here we demonstrate a general and effective strategy to fabricate a new class of three-dimensionally stretchable supercapacitors by designing a novel pyramid structure (Fig. 1). Their specific capacitances were varied by less than 7% after three-dimensional stretching for 3000 cycles. They displayed both the highest energy and power densities among the currently available stretchable supercapacitors even when the elastic substrate was not included during the calculation.

Experimental section

Patterned deposition of the catalyst

As shown in Fig. S1,† a silicon wafer was spin-coated with a 1.5 μm thick photoresist layer at 500 rpm for 5 s and then 4000 rpm for 30 s, followed by baking on a hot plate at 90 °C for 2 min to remove the solvent. The resulting wafer with the photoresist was exposed through the use of a mask under UV light for 6 s

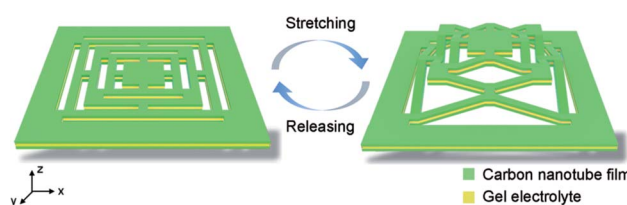


Fig. 1 Schematics of the out-of-plane deformation of a three-dimensionally stretchable supercapacitor.

^aState Key Laboratory of Molecular Engineering of Polymers, Department of Macromolecular Science and Laboratory of Advanced Materials, Fudan University, Shanghai 200438, China. E-mail: wanghj@nimte.ac.cn; penghs@fudan.edu.cn

^bKey Laboratory of Science and Technology of Eco-Textiles, Ministry of Education, Jiangnan University, Wuxi 214122, China

† Electronic supplementary information (ESI) available. See DOI: 10.1039/c6ta05545a

(wavelengths of 365 to 436 nm). Finally, it was dipped into a 2.38 wt% aqueous cleaning solution.

Preparation of the pyramid-shaped CNT film

The catalyst containing 5 nm thick Al_2O_3 and 1.2 nm thick Fe was sequentially deposited onto a silicon substrate through electron beam evaporation deposition, followed by washing with acetone. Afterward, an aligned CNT array was synthesized on the silicon in a tube furnace at 750 °C by chemical vapor deposition. Ethylene was used as the carbon source (flow rate of 30 sccm), and a mixture gas of argon (flow rate of 400 sccm) and hydrogen (flow rate of 90 sccm) served as the carrier gas.

Preparation of the CNT/PANI composite electrode

The oxygen plasma treatment was performed in oxygen microwave plasma with a flow rate of oxygen gas of 300 sccm and a pressure of 10 Pa. The reaction time ranged from 1 to 10 min with a power of 900 W. PANI was deposited onto the CNT film by electrochemical deposition through electropolymerization of aniline.²⁹ It was conducted in an aqueous solution of aniline (0.1 M) and H_2SO_4 (1 M) at a potential of 0.75 V with a three-electrode system, where platinum wire and potassium chloride-saturated Ag/AgCl functioned as the counter and reference electrodes, respectively.

Fabrication of the stretchable supercapacitor

A polyvinyl alcohol (PVA)/ H_3PO_4 gel electrolyte was prepared by dissolving 1.0 g PVA in 9.0 g deionized water at 95 °C, followed

by addition of 1.5 g H_3PO_4 aqueous solution. Two pyramid-shaped CNT films were coated with the gel electrolyte and then stacked face to face to produce a stretchable supercapacitor. The calculations of the specific capacitances are described in the ESI.†

Results and discussion

A pyramid-shaped carbon nanotube (CNT) film was synthesized by combining the patterning deposition of the catalyst and chemical vapor deposition (Fig. S1†).³⁰ Briefly, the preparation includes the patterning deposition of the catalyst and growth of the aligned CNT array, followed by pressing and peeling to form the desired CNT film (Fig. S2†). These CNT films were composed of multi-walled CNTs and were tunable from micrometers to centimeters in width and from several to tens of micrometers in thickness (Fig. S3 and S4†), which can meet the requirements for a wide range of applications. The resulting CNT film was flexible and possessed a high electrical conductivity of 10^4 S m^{-1} . This pyramid-shaped CNT film was then coated with a PVA/ H_3PO_4 gel electrolyte, followed by stacking the two as-prepared films face to face with the electrolyte sandwiched between them.

The resulting pyramid-shaped CNT film could be deformed in three dimensions. For instance, the typical pyramid-shaped CNT film could be gradually stretched along the out-of-plane direction (z axis) without obvious damage to the structure (Fig. 2a). Typically, the pyramid-shaped CNT film could be lifted in the central part with the edge standing still. The maximal

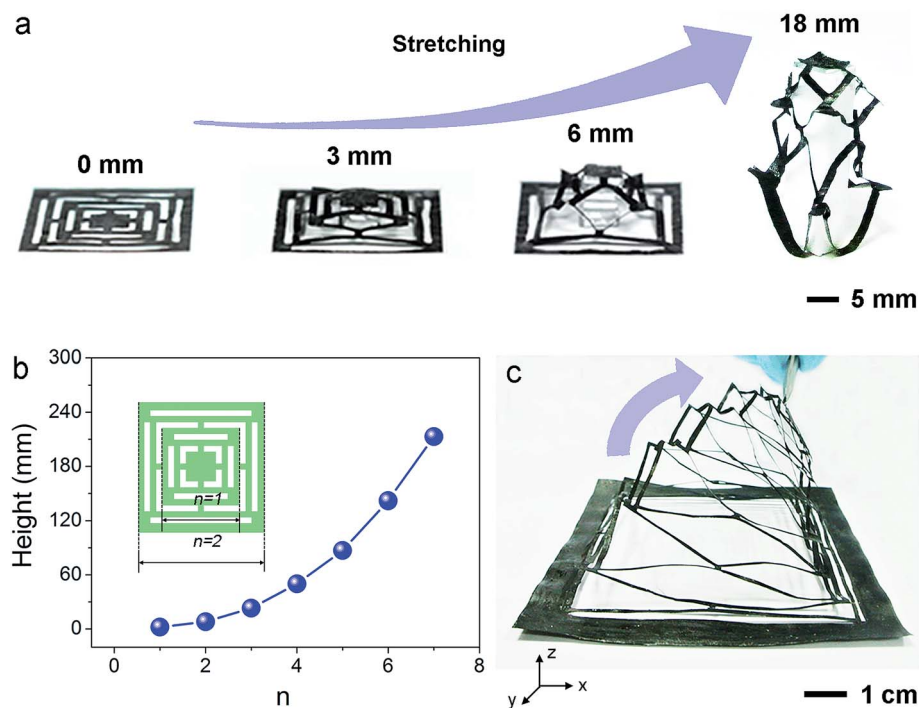


Fig. 2 Stretching property of the pyramid-shaped CNT film. (a) Photographs of a CNT film being gradually stretched along the z axis. (b) Dependence of the stretched height on the n with both the bar width and the distance between two neighboring bars as 1 mm. (c) Photograph of a pyramid-shaped CNT film under the simultaneous stretching along the x and z axes.

deformation was controlled by the structure of the pattern. To simplify the discussion, we investigated the maximally stretched height along the z axis based on the structure with a specific basic dimension of line width of the groove of 1 mm. It showed that the maximal strain along the z axis was exponentially increased with the increasing number of units n (Fig. 2b). The pyramid-shaped CNT film could also survive complex deformations with the concurrent stretching in two different directions, *e.g.*, the concurrent z - and x -axis direction (Fig. 2c).

The electronic properties were further carefully traced to quantitatively characterize the stretchability and stability of the CNT film-based electrode. It could be bent from 0 to 180° without obvious degradation of the electrical resistance (Fig. 3a). During the stretching and releasing processes along the x or z axis, the electrical resistance remained almost unchanged even after stretching at high strains (Fig. 3b and c). Even under complex deformations such as concurrent stretching along the x and z axis, it also exhibited the high stability of the resistance that was well maintained at 6.4 Ω even after 1000 stretching cycles (Fig. 3d).

The supercapacitor was then fabricated from the pyramid-shaped CNT film electrodes and PVA/H₃PO₄ gel electrolyte. We first compared the electrochemical performances of the supercapacitors with the increasing thickness of the CNT film from 8.2 to 54.4 μm, which was controlled by the growth time (Fig. S5†). The galvanostatic charge–discharge curves between 0 and 1 V at a current density of 1 mA cm⁻² were almost symmetric for all supercapacitors (Fig. S6†), which indicated

a high reversibility and coulombic efficiency during the charge and discharge processes.^{31,32} The charge–discharge time, which represents the capacitance, gradually increased with the increasing thickness of the CNT film from 8.2 to 38.3 μm, and it remained almost unchanged when the thickness was further increased to 54.4 μm due to the slightly reduced electrical resistance (Fig. S7†). Therefore, the thickness of 38.3 μm was used below unless specified otherwise.

Fig. 4a shows the electrochemical behaviors at increasing current densities. The charge–discharge curves shared a symmetrical triangular shape with the increasing current densities from 0.2 to 5 mA cm⁻², indicating a good stability over a wide range of current densities. The specific capacitances calculated from the charge–discharge curves reached an areal capacitance (C_A) of 61.4 mF cm⁻² (35.7 F g⁻¹ for gravimetric capacitance (C_M) and 16.0 F cm⁻³ for volumetric capacitance (C_V)) at a current density of 1 mA cm⁻². The cyclic voltammograms of the supercapacitors showed a typical rectangular shape, demonstrating an electrical double-layer behavior for the supercapacitor.^{33,34} The rectangular shape was well maintained with the increasing scan rate from 20 to 500 mV s⁻¹ mainly due to a low internal resistance of the supercapacitor (Fig. S8†). To further investigate the stability of the supercapacitor, cyclic charge–discharge characterization was also conducted (Fig. S9†). The supercapacitor performed stably over 10 000 cycles.

The resulting supercapacitor well maintained a high electrochemical performance under complex deformations, including bending and stretching in three dimensions. The

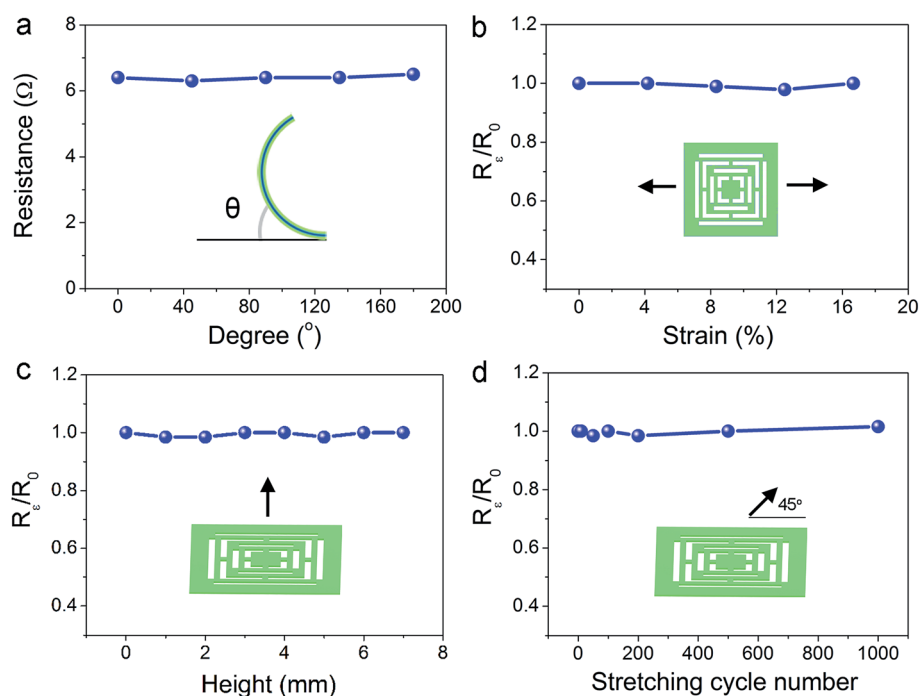


Fig. 3 Electrical properties of the pyramid-shaped CNT film. (a) Dependence of the resistance on the bending angle from 0 to 180°. (b) Dependence of the resistance ratio on the strain along the x axis. (c) Dependence of the resistance ratio on the strain along the z axis. (d) Dependence of the resistance ratio on the cycle number under the simultaneous stretching along the x and z axes with the same stretched length of 3 mm. Here R_e and R_0 correspond to the resistances before and after stretching, respectively.

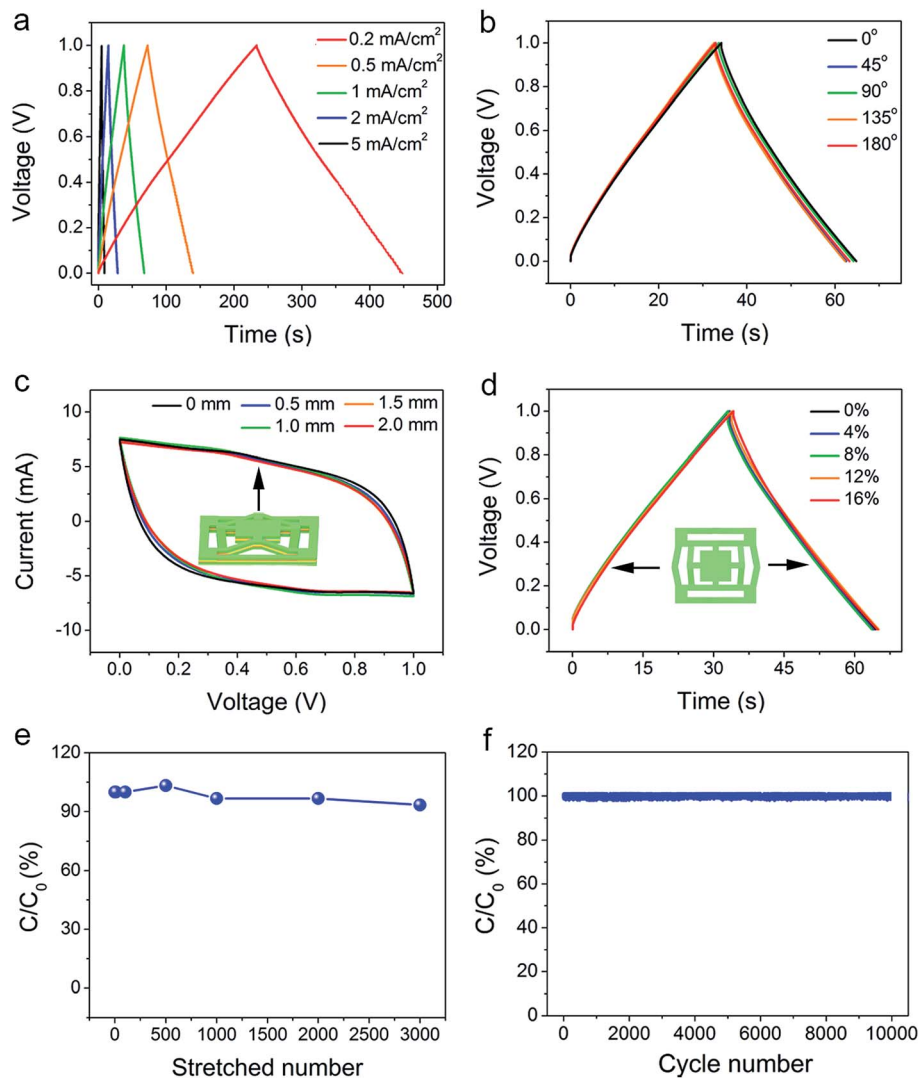


Fig. 4 Electrochemical performances of the three-dimensionally stretchable supercapacitor. (a) Galvanostatic charge–discharge profiles at increasing current densities from 0.2 to 5 mA cm⁻². (b) Galvanostatic charge–discharge profiles with increasing bending angles from 0 to 180°. (c) Cyclic voltammograms with increasing stretching heights from 0 to 2 mm along the z axis. (d) Galvanostatic charge–discharge profiles with increasing strains from 0 to 16% along the x or y axis. (e) Dependence of the specific capacitance on the stretching number with the simultaneous stretching along the x and z axes. Here C₀ and C correspond to specific capacitances before and after stretching, respectively. (f) Cyclic performance of a maximally stretched supercapacitor along the z axis.

charge–discharge curves and cyclic voltammograms were well overlapped with the increasing bending angle from 0 to 180° (Fig. 4b). The supercapacitor could also be stretched to 116% of its initial length along the x or y axis with the charge–discharge curves remaining unchanged (Fig. 4c). Due to the structural and electrical stability of the CNT film electrode, the supercapacitor could perform a three-dimensional deformation along the z axis without degradation in performance (Fig. 4d). The supercapacitor also exhibited a high stability against the repeated stretching and releasing. For instance, the specific capacitance was maintained at 93.3% after simultaneous stretching and releasing for 3000 cycles with the stretched lengths of 4 mm along the y and z axes for the typical structure (Fig. 4e). Moreover, the specific capacitances were varied below 7% after stretching to the maximal strain along the z axis for 10 000

cycles (Fig. 4f). Due to their light weight, flexibility and ventilation, these stretchable supercapacitors were particularly promising for wearable devices.

The specific capacitance reached 35.7 F g⁻¹ and could be further improved by tuning the surface nature from hydrophobic to hydrophilic due to a better permeability for the electrolyte. To this end, the as-synthesized CNT array had been first treated with oxygen plasma. Obviously, the surface properties of the resulting aligned CNTs were changed from hydrophobic with a water contact angle of 129.6° to hydrophilic with a water contact angle of almost 0° (Fig. S10†) while the surface morphology and surface roughness remained almost unchanged (Fig. S11 and S12†). As expected, the oxygen content increased with the increasing treatment time (Table S1†). The specific capacitance was first increased to 162.4 mF cm⁻² with

the increasing oxygen content to 8.26 wt% and then gradually decreased beyond this point (Fig. S13†). The decreased specific capacitance was produced by the reduced electrical conductivities of CNT films after oxygen plasma treatment, which was verified by the corresponding Nyquist plots (Fig. S14†).

The specific capacitance was further improved by introducing polyaniline (PANI), one of the most explored pseudocapacitive materials.³⁵ Owing to the hydrophilic surface of the CNT film, the aqueous solution of aniline can effectively infiltrate into the CNT film to produce the CNT/PANI composite material after electrochemical polymerization. The weight percentage of PANI could be steadily increased with the increasing deposition time and reached a high value of 60% (Fig. S15†), and all exhibited similar surface roughnesses covering at the top of CNT film (Fig. S16†). The electrochemical properties of these composite electrodes with increasing PANI weight percentages were carefully investigated at 5 mA cm^{-2} (Fig. S17 and S18†). The discharge time was gradually enhanced from 17.5 to 202.0 s with the increasing PANI from 4 to 60 wt%. For the resulting supercapacitors, the maximal C_A of 2.02 F cm^{-2} (469.9 F g^{-1} for C_M and 527.4 F cm^{-3} for C_V) occurred at 60 wt% PANI (Fig. S19†), which was approximately 33 times that of a bare CNT electrode under the same conditions. In addition, it greatly exceeds the previous stretchable supercapacitor even when the elastic polymer substrate was not included during the calculation ($7.3\text{--}335.8 \text{ F g}^{-1}$).^{10–12,36–38} The high specific capacitance accompanied both high energy density and high power output (Fig. 5). For instance, their volumetric energy densities reached $19.9 \text{ mW h cm}^{-3}$, which were higher than those of the planar supercapacitors based on PANI/CNT film electrodes³⁶ or with a stretchable electrolyte,³⁹ fiber-shaped supercapacitors derived from carbon fiber/PANI and functionalized carbon fiber electrodes⁴⁰ and thin-film lithium batteries.^{41,42} The high power density of 3.3 W cm^{-3} was also higher than those of the

commercial supercapacitors.^{43,44} Cyclic charge–discharge characterization was also conducted to further investigate its stability, and it performed stably over 20 000 cycles (Fig. S20†).

In summary, a new family of three-dimensionally stretchable supercapacitors has been created from the pyramid-shaped CNT film electrode. Compared with the previous stretchable supercapacitors that may deform in plane on elastic substrates, these pyramid-structured supercapacitors can be stretched in three dimensions with high stability even after stretching in three dimensions for thousands of cycles. They also show both higher energy and power densities compared with the other reported stretchable supercapacitors. In addition, they are breathable due to the designed grooves that produce the pyramid structure, which is particularly promising for many emerging applications such as wearable electronics. This work further provides an effective strategy for developing next-generation flexible electronic devices with high performances, e.g., three-dimensionally stretchable solar cells, batteries and sensors may be also produced based on a similar strategy.

Acknowledgements

This work was supported by the National Natural Science Foundation of China grants 21225417, 51573027 and 51403038, Science and Technology Commission of Shanghai Municipality grants 15XD1500400 and 15JC1490200 and the Program for Outstanding Young Scholars of the Organization Department of the CPC Central Committee. Part of the sample fabrication was performed at Fudan Nano-fabrication Laboratory.

References

- G. S. Jeong, D. H. Baek, H. C. Jung, J. H. Song, J. H. Moon, S. W. Hong, I. Y. Kim and S. H. Lee, *Nat. Commun.*, 2012, **3**, 977.
- W. Gao, S. Emaminejad, H. Y. Nyein, S. Challa, K. Chen, A. Peck, H. M. Fahad, H. Ota, H. Shiraki, D. Kiriya, D. H. Lien, G. A. Brooks, R. W. Davis and A. Javey, *Nature*, 2016, **529**, 509.
- S. Xu, Y. Zhang, J. Cho, J. Lee, X. Huang, L. Jia, J. A. Fan, Y. Su, J. Su, H. Zhang, H. Cheng, B. Lu, C. Yu, C. Chuang, T. I. Kim, T. Song, K. Shigeta, S. Kang, C. Dagdeviren, I. Petrov, P. V. Braun, Y. Huang, U. Paik and J. A. Rogers, *Nat. Commun.*, 2013, **4**, 1543.
- Z. Liu, Z. S. Wu, S. Yang, R. Dong, X. Feng and K. Mullen, *Adv. Mater.*, 2016, **28**, 2217.
- D. Kim, D. Kim, H. Lee, Y. R. Jeong, S. J. Lee, G. Yang, H. Kim, G. Lee, S. Jeon, G. Zi, J. Kim and J. S. Ha, *Adv. Mater.*, 2016, **28**, 748.
- F. W. Li, J. T. Chen, X. S. Wang, M. Q. Xue and G. F. Chen, *Adv. Funct. Mater.*, 2015, **25**, 4601.
- Z. M. Song, X. Wang, C. Lv, Y. H. An, M. B. Liang, T. Ma, D. He, Y. J. Zheng, S. Q. Huang, H. Y. Yu and H. Q. Jiang, *Sci. Rep.*, 2015, **5**, 10988.
- Y. Huang, M. Zhong, Y. Huang, M. S. Zhu, Z. X. Pei, Z. F. Wang, Q. Xue, X. M. Xie and C. Y. Zhi, *Nat. Commun.*, 2015, **6**, 10310.

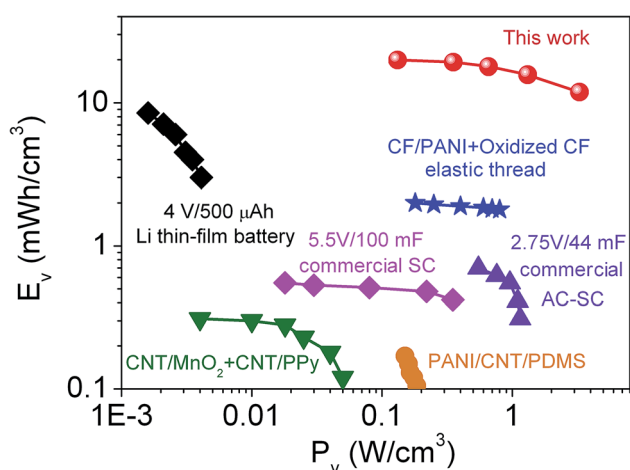


Fig. 5 Comparison of the three-dimensionally stretchable supercapacitor fabricated from the aligned CNT/PANI composite electrode (60 wt% of PANI) with the other stretchable supercapacitors and commercial energy storage devices in volumetric energy and power densities.^{31–36} Here CF, AC, SC, PPy and PDMS correspond to carbon fiber, activated carbon, supercapacitor, polypyrrole and poly(dimethylsiloxane), respectively.

- 9 D. Qi, Z. Liu, Y. Liu, W. R. Leow, B. Zhu, H. Yang, J. Yu, W. Wang, H. Wang, S. Yin and X. Chen, *Adv. Mater.*, 2015, **27**, 5559.
- 10 T. Chen, Y. Xue, A. K. Roy and L. Dai, *ACS Nano*, 2014, **8**, 1039.
- 11 T. Chen, H. Peng, M. Durstock and L. Dai, *Sci. Rep.*, 2014, **4**, 3612.
- 12 C. J. Yu, C. Masarapu, J. P. Rong, B. Q. Wei and H. Q. Jiang, *Adv. Mater.*, 2009, **21**, 4793.
- 13 J. Lee, W. Kim and W. Kim, *ACS Appl. Mater. Interfaces*, 2014, **6**, 13578.
- 14 M. Kaltenbrunner, M. S. White, E. D. Glowacki, T. Sekitani, T. Someya, N. S. Saticiftci and S. Bauer, *Nat. Commun.*, 2012, **3**, 770.
- 15 Y. Huang, J. Tao, W. Meng, M. Zhu, Y. Huang, Y. Fu, Y. Gao and C. Zhi, *Nano Energy*, 2015, **11**, 518.
- 16 T. C. Shyu, P. F. Damasceno, P. M. Dodd, A. Lamoureux, L. Xu, M. Shlian, M. Shtein, S. C. Glotzer and N. A. Kotov, *Nat. Mater.*, 2015, **14**, 785.
- 17 L. Kou, T. Huang, B. Zheng, Y. Han, X. Zhao, K. Gopalsamy, H. Sun and C. Gao, *Nat. Commun.*, 2014, **5**, 3754.
- 18 K. Jang, S. Y. Han, S. Xu, K. E. Mathewson, Y. Zhang, J.-W. Jeong, G.-T. Kim, R. C. Webb, J. W. Lee, T. J. Dawidczyk, R. H. Kim, Y. M. Song, W.-H. Yeo, S. Kim, H. Cheng, S. I. Rhee, J. Chung, B. Kim, H. U. Chung, D. Lee, Y. Yang, M. Cho, J. G. Gaspar, R. Carbonari, M. Fabiani, G. Gratton, Y. Huang and J. A. Rogers, *Nat. Commun.*, 2014, **5**, 4779.
- 19 L. Liu, Y. Yu, C. Yan, K. Li and Z. Zheng, *Nat. Commun.*, 2015, **6**, 7260.
- 20 J. A. Fan, W.-H. Yeo, Y. Su, Y. Hattori, W. Lee, S.-Y. Jung, Y. Zhang, Z. Liu, H. Cheng, L. Falgout, M. Bajema, T. Coleman, D. Gregoire, R. J. Larsen, Y. Huang and J. A. Rogers, *Nat. Commun.*, 2014, **5**, 3266.
- 21 K.-I. Jang, H. U. Chung, S. Xu, C. H. Lee, H. Luan, J. Jeong, H. Cheng, G. Kim, S. Y. Han, J. W. Lee, J. Kim, M. Cho, F. Miao, Y. Yang, H. N. Jung, M. Flavin, H. Liu, G. W. Kong, K. J. Yu, S. I. Rhee, J. Chung, B. Kim, J. W. Kwak, M. H. Yun, J. Y. Kim, Y. M. Song, U. Paik, Y. Zhang, Y. Huang and J. A. Rogers, *Nat. Commun.*, 2015, **6**, 6566.
- 22 M. K. Blees, A. W. Barnard, P. A. Rose, S. P. Roberts, K. L. McGill, P. Y. Huang, A. R. Ruyack, J. W. Kevek, B. Kobrin, D. A. Muller and P. L. McEuen, *Nature*, 2015, **524**, 204.
- 23 B. Y. Ahn, E. B. Duoss, M. J. Motala, X. Y. Guo, S. I. Park, Y. J. Xiong, J. Yoon, R. G. Nuzzo, J. A. Rogers and J. A. Lewis, *Science*, 2009, **323**, 1590.
- 24 J. H. Lee, C. Y. Koh, J. P. Singer, S. J. Jeon, M. Maldovan, O. Stein and E. L. Thomas, *Adv. Mater.*, 2014, **26**, 532.
- 25 H. Zhang, X. Yu and P. V. Braun, *Nat. Nanotechnol.*, 2011, **6**, 277.
- 26 W. Huang, X. Yu, P. Froeter, R. Xu, P. Ferreira and X. Li, *NanoLett.*, 2012, **12**, 6283.
- 27 K. Sun, T. S. Wei, B. Y. Ahn, J. Y. Seo, S. J. Dillon and J. A. Lewis, *Adv. Mater.*, 2013, **25**, 4539.
- 28 S. Xu, Z. Yan, K. I. Jang, W. Huang, H. R. Fu, J. Kim, Z. Wei, M. Flavin, J. McCracken, R. Wang, A. Badea, Y. Liu, D. Q. Xiao, G. Y. Zhou, J. Lee, H. U. Chung, H. Y. Cheng, W. Ren, A. Banks, X. L. Li, U. Paik, R. G. Nuzzo, Y. G. Huang, Y. H. Zhang and J. A. Rogers, *Science*, 2015, **347**, 154.
- 29 S. Zeng, H. Chen, F. Cai, Y. Kang, M. Chen and Q. Li, *J. Mater. Chem. A*, 2015, **3**, 23864.
- 30 L. Qiu, X. Sun, Z. Yang, W. Guo and H. Peng, *Acta Chim. Sin.*, 2012, **70**, 1523.
- 31 Y. W. Zhu, S. Murali, M. D. Stoller, K. J. Ganesh, W. W. Cai, P. J. Ferreira, A. Pirkle, R. M. Wallace, K. A. Cychoz, M. Thommes, D. Su, E. A. Stach and R. S. Ruoff, *Science*, 2011, **332**, 1537.
- 32 X. Yang, J. Zhu, L. Qiu and D. Li, *Adv. Mater.*, 2011, **23**, 2833.
- 33 P. Simon and Y. Gogotsi, *Nat. Mater.*, 2008, **7**, 845.
- 34 D. Pech, M. Brunet, H. Durou, P. Huang, V. Mochalin, Y. Gogotsi, P. L. Taberna and P. Simon, *Nat. Nanotechnol.*, 2010, **5**, 651.
- 35 K. Wang, Q. Meng, Y. Zhang, Z. Wei and M. Miao, *Adv. Mater.*, 2013, **25**, 1494.
- 36 Z. Niu, H. Dong, B. Zhu, J. Li, H. H. Hng, W. Zhou, X. Chen and S. Xie, *Adv. Mater.*, 2013, **25**, 1058.
- 37 X. Chen, H. Lin, P. Chen, G. Guan, J. Deng and H. Peng, *Adv. Mater.*, 2014, **26**, 4444.
- 38 M. Yu, Y. Zhang, Y. Zeng, M. Balogun, K. Mai, Z. Zhang, X. Lu and Y. Tong, *Adv. Mater.*, 2014, **26**, 4724.
- 39 Q. Tang, M. Chen, C. Yang, W. Wang, H. Bao and G. Wang, *ACS Appl. Mater. Interfaces*, 2015, **7**, 15303.
- 40 H. Jin, L. Zhou, C. Mak, H. Huang, W. M. Tang and H. L. W. Chan, *Nano Energy*, 2015, **11**, 662.
- 41 M. F. El-Kady, V. Strong, S. Dubin and R. B. Kaner, *Science*, 2012, **335**, 1326.
- 42 Z. S. Wu, K. Parvez, X. Feng and K. Mullen, *Nat. Commun.*, 2013, **4**, 2487.
- 43 D. Pech, M. Brunet, H. Durou, P. Huang, V. Mochalin, Y. Gogotsi, P. L. Taberna and P. Simon, *Nat. Nanotechnol.*, 2010, **5**, 651.
- 44 D. Yu, K. Goh, H. Wang, L. Wei, W. Jiang, Q. Zhang, L. Dai and Y. Chen, *Nat. Nanotechnol.*, 2014, **9**, 555.